

Coherent charge transport through molecular wires: “Exciton blocking” and current from electronic excitations in the wire

GuangQi Li,¹ Boris D. Fainberg,^{1,2,*} Abraham Nitzan,¹ Sigmund Kohler,³ and Peter Hänggi⁴

¹*Raymond and Beverly Sackler Faculty of Exact Sciences,*

School of Chemistry, Tel-Aviv University, Tel-Aviv 69978, Israel

²*Faculty of Sciences, Holon Institute of Technology, 52 Golomb St., Holon 58102, Israel*

³*Instituto de Ciencia de Materiales de Madrid (CSIC), Cantoblanco, 28049 Madrid, Spain*

⁴*Institute for Physics, University of Augsburg, Augsburg, D-86135, Germany*

(Dated: February 22, 2024)

We consider exciton effects on current in molecular nanojunctions, using a model comprising a two two-level sites bridge connecting free electron reservoirs. Expanding the density operator in the many-electron eigenstates of the uncoupled sites, we obtain a 16×16 density matrix in the bridge subspace whose dynamics is governed by Liouville equation that takes into account interactions on the bridge as well as electron injection and damping to and from the leads. Our consideration can be considerably simplified by using the pseudospin description based on the symmetry properties of Lie group $SU(2)$. We study the influence of the bias voltage, the Coulomb repulsion and the energy-transfer interactions on the steady-state current and in particular focus on the effect of the excitonic interaction between bridge sites. Our calculations show that in case of non-interacting electrons this interaction leads to reduction in the current at high voltage for a homodimer bridge. In other words, we predict the effect of “exciton” blocking. The effect of “exciton” blocking is modified for a heterodimer bridge, and disappears for strong Coulomb repulsion at sites. In the latter case the exciton type interactions can open new channels for electronic conduction. In particular, in the case of strong Coulomb repulsion, conduction exists even when the electronic connectivity does not exist.

PACS numbers: 73.63.Rt, 73.23.Hk, 73.22.Lp

I. INTRODUCTION

Electron transport through molecular wires has been under intense theoretical (see e.g. [1, 2]) and experimental (see e.g. [3, 4]) study in the last few years. Theoretical studies usually fall into two categories. The first focuses on the *ab-initio* computations of the orbitals relevant for the motion of excess charges through the molecular wire [5–9], while the other [10, 11] employs generic models to gain qualitative understanding of the transport process. At the simplest level [10, 11] the wire Hamiltonian is described by a tight-binding chain composed of N sites with nearest-neighbor coupling (Huckel model) that represents the electron transfer (tunneling) interactions between adjacent sites. This model has been generalized to include Coulomb interactions between electrons on the same site [12] (Hubbard model) and/or electron-phonon interactions [13]. In the present paper we investigate another extension of this model, in which we take into account energy transfer interactions between adjacent molecular sites.

Energy-transfer interactions - excitation (deexcitation) of a site accompanied by deexcitation (excitation) of another are well-known in the exciton theory [14–16]. In particular, Frenkel excitons - neutral excited states in which an electron and a hole are placed on the same site are readily transferred between sites, and such intersite

interactions can accompany the charge transfer processes as was shown for charge-transfer excitons [17] in (quasi-) one-dimensional structures [18, 19], including polysilanes [20–22]. The latter show a weak coupling between the Frenkel exciton with the admixture of charge transfer states and nuclear motions [21, 22].

In molecular bridges energy-transfer interactions can also sometimes have important effects on charge transfer dynamics. Charge and energy transfer in a linear 2,2':6',2"-terpyridine-based trinuclear Ru-(II)-Os(II) nanometer-sized array [23], and one-dimensional energy/electron transfer of amylose-encapsulated chain chromophores [24] are examples. In addition, it seems likely that energy transfer takes place in chemically responsive molecular transistors based on a dimer of terpyridyl molecules combined with ion Co^{2+} [25].

It should be noted that electron transfer is a tunneling process that depends exponentially on the site-site distance, while energy transfer is associated with dipolar coupling that scales like the inverse cube of this distance, and can therefore dominate at larger distances. The importance of the latter stems also from geometric issues, which are related to the dipole-dipole interaction between different sites occurring in the vicinity of metal particles in molecular nanojunctions. Really, Gersten and Nitzan [26, 27] predicted accelerated dipole-dipole energy transfer near a solid particle (see also [28, 29]), and in the last time a number of works devoted to the exciton-plasmon interactions have been published [30–33] that are related to physical effects due to the local field enhancement [34–39].

*Electronic address: fainberg@hit.ac.il

How will such dipolar interactions affect the conduction properties of molecular junctions? This question was addressed by Galperin, Nitzan and Ratner by the example of a junction composed of one-site-wire and two metal leads [40], where they predicted the existence of non-Landauer current induced by the electron-hole excitations in the leads. To the best of our knowledge, there were no analog treatment of simultaneous electron and energy transfer (excitons) in multisite bridges. Here we address this problem by using the Liouville-von Neumann equation (LNE) for the total density operator to derive an expression for the conduction of a molecular wire model that contains both electron and energy-transfer interactions. While not a central issue of the present work, we note that energy transfer is closely related to heat transfer through the molecular nanojunction - an issue of important consequences for junction stability and integrity.

Treated separately, the simplest models of exciton and electron transport may be represented by tight-binding transport models, albeit in different representations. Indeed, in the wire Hamiltonian (see Eq.(3) below), both the electron- and energy-transfer terms are binary in terms of the annihilation and creation operators for electrons and excitons, respectively. Their simultaneous treatment, however, constitutes a rather complex non-linear problem. In this work we combine a tight-binding model for electron transport [10, 11] with that of one-dimensional Frenkel excitons [14–16] to investigate the effect of energy transfer interaction on electron transport in one-dimensional nanowires. The outline of the paper is as follows. In Sec.II we introduce our model and in Sec.III we derive a master equation in the eigenbasis of many-electron wire Hamiltonian. Sec.IV is devoted to the analytical solution of the problem where we consider both non-interacting electrons at a site and strong Coulomb repulsion at sites. In Sec.V we show that the exciton type interactions can open new channels for electronic conduction. In Sec.VI we carry out numerical simulations, compare them with the analytical theory and show the existence of the “exciton blocking” effect. We summarize our results in Sec.VII. In Appendix A we calculate the eigenbasis of many-electron wire Hamiltonian for non-interacting electrons at a site, using the Jordan-Wigner transformation [41]. In Appendix B we present auxiliary calculations.

II. MODEL

We consider a spinless model for a molecular wire that comprises two interacting sites, each represented by its ground, $|g\rangle$, and excited, $|e\rangle$, states positioned between two leads represented by free electron reservoirs L and R (Fig.1). The electron reservoirs (leads) are characterized by their electronic chemical potentials μ_L and μ_R , where the difference $\mu_L - \mu_R = eV_{bs}$ is the imposed voltage bias. The corresponding Hamiltonian is

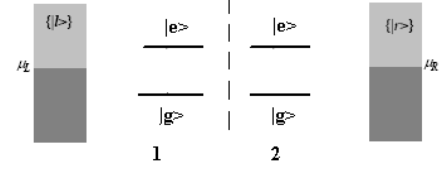


FIG. 1: A model for energy-transfer induced effects in molecular conduction. The right ($R = |\{r\}\rangle$) and left ($L = |\{l\}\rangle$) manifolds represent two metal leads characterized by electrochemical potentials μ_R and μ_L respectively, each coupled to its nearest molecular site. The molecular bridge is a dimer, where each site is represented by its ground, $|1g\rangle$ and $|2g\rangle$, and excited, $|1e\rangle$ and $|2e\rangle$, states.

$$\hat{H} = \hat{H}_{wire} + \hat{H}_{leads} + \hat{H}_{contacts} \quad (1)$$

$$\hat{H}_{leads} = \sum_{k \in \{L, R\}} \varepsilon_k \hat{c}_k^+ \hat{c}_k \quad (2)$$

$$\begin{aligned} \hat{H}_{wire} = & \sum_{\substack{m=1,2 \\ f=g,e}} \varepsilon_{mf} \hat{c}_{mf}^+ \hat{c}_{mf} - \sum_{f=g,e} \Delta_f (\hat{c}_{2f}^+ \hat{c}_{1f} + \hat{c}_{1f}^+ \hat{c}_{2f}) + \\ & + \hbar J (b_1^+ b_2 + b_2^+ b_1) + \sum_{m=1,2} U_m N_m (N_m - 1) \end{aligned} \quad (3)$$

$$\hat{H}_{contacts} = \hat{V} + \hat{W} \quad (4)$$

$$\hat{V} = \sum_{mf} \hat{V}_{mf} = \sum_{mf, k \in K_m} V_k^{(mf)} \hat{c}_k^+ \hat{c}_{mf} + H.c., \quad (5)$$

$$\hat{W} = \sum_m \hat{W}_m = \sum_{m, k \neq k' \in K_m} \hat{W}_{kk'}^{(m)} b_{k'k}^+ b_m + H.c., \quad (6)$$

where \hat{c}_{mf}^+ (\hat{c}_{mf}) ($m = 1, 2, f = g, e$) are creation (annihilation) operators for electrons in the different site states of energies ε_{mf} , while \hat{c}_k^+ (\hat{c}_k) ($k \in L, R$) are creation (annihilation) operators for free electrons (energies ε_k) in the leads L and R . $\hat{n}_{mf} = \hat{c}_{mf}^+ \hat{c}_{mf}$ are the occupation operators for the different site states, and site occupation operators are given by $N_m = \hat{n}_{mg} + \hat{n}_{me}$. The operators $b_m^+ = \hat{c}_{me}^+ \hat{c}_{mg}$ and $b_m = \hat{c}_{mg}^+ \hat{c}_{me}$ are excitonic (creation and annihilation) operators on the molecular sites $m = 1, 2$, while $b_{k'k}^+ = \hat{c}_k^+ \hat{c}_{k'}$ ($k, k' \in L$ or R) corresponds to electron-hole pairs in the leads. In the wire Hamiltonian, Eq. (3), the Δ_f terms represent electron hopping between site states of similar energies (i.e.

between $|g\rangle$ and between $|e\rangle$ states of adjacent molecular sites), the J terms represent exciton hopping (energy transfer) between molecular sites and the U terms correspond to on-site Coulomb interactions. The molecular-lead interactions $\hat{H}_{contacts}$ are taken to account for two physical processes: \hat{V} describes electron transfer between the molecular bridge and the leads that gives rise to net current in the biased junction, while \hat{W} describes energy transfer between the bridge and electron-hole excitations in the leads. In (5) and (6) K_m is the lead closer the the molecular site m ($K_1 = L$, $K_2 = R$) and $H.c.$ denotes Hermitian conjugate. In what follows it will be useful also to define the population operators

$$\lambda_f = \hat{n}_{2f} + \hat{n}_{1f} \quad (7)$$

in the manifolds of ground ($f = g$) and excited ($f = e$) site levels.

We consider electronic transport through the molecular wire where the leads $K = L, R$ are taken to be each in its own equilibrium characterized by its temperature T (here taken equal for the two leads) and electronic electrochemical potential μ_K . Therefore, the lead electrons are described by the equilibrium Fermi functions $f_K(\varepsilon_k) = [\exp((\varepsilon_k - \mu_K)/k_B T) + 1]^{-1}$. Consequently expectation values for lead operators can be traced back to the expression $\langle \hat{c}_k^\dagger \hat{c}_{k'} \rangle = f_K(\varepsilon_k) \delta_{kk'}$ where $\delta_{kk'}$ is the Kronecker delta. The excitonic operators are equal to $b_m^+ = \hat{c}_{me}^+ \hat{c}_{mg}$. The effect of the corresponding interaction in the bridge ($= \hbar J b_1^+ b_2 + H.c.$) on the charge transport properties is the subject of our discussion.

III. MASTER EQUATION

Our analysis is based on the LNE, or the generalized master equation for the reduced density matrix of the molecular subsystem, obtained using a standard procedure [10, 11, 42] based on taking $\hat{H}_{contacts}$ as a perturbation. Briefly, one starts with the LNE for the total density operator and use the projectors of the type $P_K \rho(t) = \rho_K Tr_K \rho(t)$ in order to derive an equation for the time evolution of the reduced density matrix $\sigma = Tr_R Tr_L \rho$. The calculation is facilitated by invoking the so called non-crossing approximation that assumes that the effects of different reservoirs (here L, R) and different relaxation processes (here \hat{V}, \hat{W}) are independent and additive. This leads to

$$\begin{aligned} \frac{d\sigma(t)}{dt} = & -\frac{i}{\hbar} [\hat{H}_{wire}, \sigma(t)] - \\ & -\frac{1}{\hbar^2} Tr_K \int_0^\infty dx [\hat{V}, [\hat{V}^{int}(-x), \rho(t)]] \\ & -\frac{1}{\hbar^2} Tr_K \int_0^\infty dx [\hat{W}, [\hat{W}^{int}(-x), \rho(t)]] \quad (8) \end{aligned}$$

where for any operator \hat{O} , \hat{O}^{int} is the corresponding interaction representation

$$\begin{aligned} \hat{O}^{int}(-x) = & \exp[-\frac{i}{\hbar} (\hat{H}_{wire} + \hat{H}_{leads})x] \\ & \hat{O} \exp[\frac{i}{\hbar} (\hat{H}_{wire} + \hat{H}_{leads})x] \quad (9) \end{aligned}$$

and where $Tr_K = Tr_L Tr_R$.

Consider first terms with the electron transfer interactions \hat{V} . Writing the coupling Hamiltonians \hat{V}_{nf} (Eq.(5)) as

$$\hat{V}_{nf} = \hat{c}_{nf} \Lambda_{nf}^+ + \hat{c}_{nf}^+ \Lambda_{nf} \quad (10)$$

where $\Lambda_{nf} = \sum_{k \in K_n} V_k^{(nf)} \hat{c}_k$, we have $\hat{V}_{nf}^{int}(-x) = \hat{c}_{nf}^{+int}(-x) \Lambda_{nf}^{int}(-x) + \hat{c}_{nf}^{int}(-x) \Lambda_{nf}^{+int}(-x)$ with $\Lambda_{nf}^{int}(-x) = \sum_{k \in K_n} V_k^{(nf)} \hat{c}_k \exp(\frac{i}{\hbar} \varepsilon_k x)$.

Similarly, writing the coupling Hamiltonian for energy transfer $\hat{W} = \sum_n \hat{W}_n$ as

$$\hat{W}_n = b_n^+ \Theta_n + b_n \Theta_n^+ \quad (11)$$

where $\Theta_n = \sum_{k \neq k' \in K_n} W_{kk'}^{(n)} b_{k'k}$, then

$$\hat{W}_n^{int}(-x) = b_n^{+int}(-x) \Theta_n^{int}(-x) + b_n^{int}(-x) \Theta_n^{+int}(-x) \quad (12)$$

where

$$\Theta_n^{int}(-x) = \sum_{k \neq k' \in K_n} W_{kk'}^{(n)} b_{k'k} \exp[\frac{i}{\hbar} (\varepsilon_{k'} - \varepsilon_k)x] \quad (13)$$

Bearing in mind that $\rho(t) = \sigma(t) \rho_K$ where $\sigma(t) = Tr_K \rho(t)$ and Eqs.(10), (11) and (12), we get for the second term on the RHS of Eq.(8)

$$\begin{aligned} & -\frac{1}{\hbar^2} Tr_K \left\{ \int_0^\infty dx [\hat{V}, [\hat{V}^{int}(-x), \rho(t)]] \right\} = \\ & -\frac{1}{\hbar^2} \int_0^\infty dx \{ Tr_K [\hat{V} \hat{V}^{int}(-x) \rho_K] \sigma(t) \\ & - Tr_K [\hat{V} \rho_K \sigma(t) \hat{V}^{int}(-x)] - Tr_K [\hat{V}^{int}(-x) \rho_K \sigma(t) \hat{V}] \\ & + Tr_K [\rho_K \sigma(t) \hat{V}^{int}(-x) \hat{V}] \} \quad (14) \end{aligned}$$

In evaluating the RHS of Eq.(14) we encounter reservoir correlation functions that reflect the reservoir equilibrium properties as well as the nature of its interaction with the wire. For example,

$$\begin{aligned} C_{nf}(-x) = & Tr_K [\Lambda_{nf} \Lambda_{nf}^+(-x) \rho_{K_n}] \\ = & \sum_{k \in K_n} |V_k^{(nf)}|^2 [1 - f_{K_n}(\varepsilon_k)] \exp(-\frac{i}{\hbar} \varepsilon_k x) \quad (15) \end{aligned}$$

Turning to the energy transfer contribution, third term on the RHS of Eq.(8), we obtain an expression of the form (14) with the energy transfer interaction \hat{W} replacing \hat{V} . Using the Wick's theorem, we obtain correlation functions of the type

$$\begin{aligned}
D_n(-x) &= Tr_K[\Theta_n \Theta_n^+(-x) \rho_{K_n}] \\
&= \sum_{k \neq k' \in K_n} \left| W_{kk'}^{(n)} \right|^2 f_{K_n}(\varepsilon_k) [1 - f_{K_n}(\varepsilon_{k'})] \exp\left[\frac{i}{\hbar}(\varepsilon_k - \varepsilon_{k'})x\right]
\end{aligned} \tag{16}$$

Below we get a Markovian master equation in the wide-band limit. The full master equation obtained in this way constitutes a set of 256 coupled equations for the 16x16 elements of the wire density matrix, which can be solved numerically by diagonalizing the corresponding Liouvillian matrix. In particular we are interested in the steady state solution, σ_{SS} , which is given by the eigenvector of zero eigenvalue. Once σ_{SS} has been found, the current is obtained from

$$\langle I \rangle = Tr(\hat{I} \sigma_{SS}) \tag{17}$$

where the current operator (defined, e.g., as the rate of change of electron population on the left of the dashed line in Fig. 1) is given by

$$\hat{I} = e \frac{d}{dt} \hat{N} = \frac{ie}{\hbar} [\hat{H}, \hat{N}] \tag{18}$$

$$\hat{N} = \sum_{k \in L} \hat{c}_k^\dagger \hat{c}_k + \hat{n}_{1g} + \hat{n}_{1e} \tag{19}$$

In section VI we show some results of such numerical calculations. To gain better insight of the transport properties of this model, analytical simplifications in some limits are useful. These are discussed next.

IV. ANALYTICAL EVALUATION

It is known [11] that for the evaluation of Eqs. (8) and (14) it is essential to work in the representation of the eigenstates of the Hamiltonian $\hat{H}_{wire} + \hat{H}_{leads}$ that defines the zeroth-order time evolution. The use of other representations bears the danger of generating artifacts, which, for instance, may lead to a violation of fundamental equilibrium properties [43]. We thus face the problem of diagonalizing a matrix of order 256. This procedure may be facilitated by using the pseudospin description based on the symmetry properties of Lie group $SU(2)$ associated with the two state problem ($1f, 2f$); $f = e, g$. Such a “donor acceptor” system may be described by the “charge transfer” operators $b_f^+ = \hat{c}_{2f}^\dagger \hat{c}_{1f}$ and $b_f = \hat{c}_{1f}^\dagger \hat{c}_{2f}$ that describe intersite charge transfer $1 \rightarrow 2$ and $2 \rightarrow 1$, respectively, in upper and lower states of the molecular dimer. The non-diagonal part of \hat{H}_{wire} , Eq.(3), can then be written in terms of operators b_f only

$$\hat{H}_{wire}^{(nondiag)} = - \sum_{f=g,e} \Delta_f (b_f^+ + b_f) - \hbar J (b_e^+ b_g + b_g^+ b_e) \tag{20}$$

Define also the pseudospin (Bloch) vector in the second quantization picture

$$\begin{pmatrix} r_1^f \\ r_2^f \\ r_3^f \end{pmatrix} = \begin{pmatrix} b_f^+ + b_f \\ i(b_f - b_f^+) \\ \hat{n}_{2f} - \hat{n}_{1f} \end{pmatrix}; \quad f = g, e \tag{21}$$

Its components have the following properties: (a) They satisfy the same commutation rules as Pauli matrices $\hat{\sigma}_{1,2,3}$ [44–46]; (b) the operators $\lambda_f = \hat{n}_{2f} + \hat{n}_{1f} = \sum_{m=1,2} \hat{c}_{mf}^\dagger \hat{c}_{mf}$, $f = e, g$ (cf. Eq.(7)) and r_i^f commute: $[r_i^f, \lambda_f] = 0$ ($i = 1, 2, 3$); (c) any linear operator of the “donor acceptor” system can be written as linear superposition of the operators $\{r_i^f\}$ and λ_f . In particular, the wire Hamiltonian can be written as

$$\begin{aligned}
\hat{H}_{wire} &= \frac{1}{2} \lambda_e (\varepsilon_{1e} + \varepsilon_{2e}) + \sum_{f=g,e} \left[\frac{1}{2} r_3^f (\varepsilon_{2f} - \varepsilon_{1f}) - \Delta_f r_1^f \right] \\
&\quad - \frac{\hbar J}{2} (r_1^e r_1^g + r_2^e r_2^g) + \sum_{m=1,2} U_m N_m (N_m - 1) \tag{22}
\end{aligned}$$

In Eq.(22) we have put, without loss of generality, $(\varepsilon_{1g} + \varepsilon_{2g})/2 = 0$. Because the operators λ_f and r_i^f commute, λ_f is conserved under unitary transformations related to the diagonalization of \hat{H}_{wire} . Therefore, a total $2^4 \times 2^4$ space can be partitioned into nine smaller subspaces, i.e. the Liouvillian matrix in the required basis is block diagonal with blocks, according to the values of $\lambda_f = 0, 1, 2$ (see Fig.2): four one-dimensional subspaces for $\lambda_f = 0, 2$ for either $f = e, g$ (type I); four two-dimensional subspaces for $\lambda_f = 1$ and $\lambda_{f'} = 0, 2$ where $f \neq f'$ (type II); and one four-dimensional subspace for $\lambda_e = \lambda_g = 1$ (type III). The type I submatrix is diagonal, while four state pairs with each pair coupled by the charge transfer interaction are associated with the four 2×2 blocks of the type II subspace. The remaining four states are coupled by both the charge transfer and exciton transfer interaction and constitute the 4×4 block of subspace III. Each of these subspaces is characterized by assigning the values (λ_e, λ_g) of total populations in the ground and excited states of the two bridge sites.

Using the identity

$$(r_1^f)^2 = (r_2^f)^2 = (r_3^f)^2 = \lambda_f - 2\hat{n}_{2f}\hat{n}_{1f} = \begin{cases} 0 & \text{for } \lambda_f = 0, 2 \\ 1 & \text{for } \lambda_f = 1 \end{cases}, \tag{23}$$

the wire Hamiltonian (22) can be written in the form

$$\begin{aligned}
\hat{H}_{wire} &= \frac{1}{2} \lambda_e (\varepsilon_{1e} + \varepsilon_{2e}) + \sum_{m=1,2} U_m N_m (N_m - 1) + \\
&\quad + 0 \quad \text{For subspaces I} \\
&\quad + \frac{1}{2} r_3^f (\varepsilon_{2f} - \varepsilon_{1f}) - \Delta_f r_1^f \quad \text{For subspaces II} \\
&\quad + \left[\frac{1}{2} \sum_{f=g,e} r_3^f (\varepsilon_{2f} - \varepsilon_{1f}) - \sum_{f=g,e} \Delta_f r_1^f - \right. \\
&\quad \left. - \frac{\hbar J}{2} (r_1^e r_1^g + r_2^e r_2^g) \right] \quad \text{For subspace III}
\end{aligned} \tag{24}$$

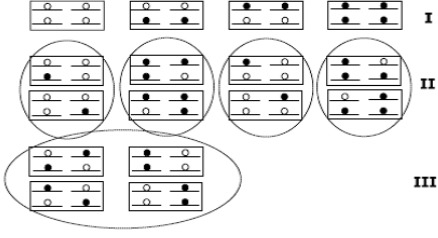


FIG. 2: A schematic display of the block structure of the wire Hamiltonian.

This prediagonalization provides an important simplification of our problem. From Eqs. (17), (18), (19) the current is given by

$$\hat{I} = \frac{ie}{\hbar} \sum_{f=g,e} \Delta_f (b_f - b_f^\dagger) = \frac{e}{\hbar} \sum_{f=g,e} \Delta_f r_2^f \quad (25)$$

Using Eq.(23), this yields

$$\hat{I} = \frac{e}{\hbar} \sum_{f=g,e} \Delta_f r_2^f (\lambda_f = 1) \quad (26)$$

Obviously $\lambda_f = 1$ in Eq.(26) is another way of saying

$$\begin{aligned} \langle \alpha | \hat{c}_{nf}^{int}(-x) | \beta \rangle &= [\hat{Y}^+(\lambda_e(\alpha), \lambda_g(\alpha)) \tilde{\chi}^+(\lambda_e(\alpha), \lambda_g(\alpha)) \hat{c}_{nf} \tilde{\chi}(\lambda_e(\beta), \lambda_g(\beta)) \hat{Y}(\lambda_e(\beta), \lambda_g(\beta))]_{\alpha\beta} \\ &\times \exp\left[\frac{i}{\hbar} (E_\beta(\lambda_e(\beta), \lambda_g(\beta)) - E_\alpha(\lambda_e(\alpha), \lambda_g(\alpha)))x\right] \end{aligned}$$

where $(\lambda_e(\alpha), \lambda_g(\alpha))$ denotes the subspace associated with the eigenstate α and points to the corresponding values of λ_e and λ_g , and where $(\lambda_e(\beta), \lambda_g(\beta)) = (\lambda_e(\alpha) + 1, \lambda_g(\alpha))$ if $f = e$ and $(\lambda_e(\beta), \lambda_g(\beta)) = (\lambda_e(\alpha), \lambda_g(\alpha) + 1)$

that the current in channel f exists only for the case of one of states $\{f\}$ is occupied and another one of $\{f\}$ is unoccupied.

Further simplification is made below, when we consider two specific limiting cases. The first limit, $U_m = 0$, describes noninteracting electrons at each sites. In the opposite limit with strong on-site Coulomb repulsion U_m ($m = 1, 2$) is much larger than any other energy scale of the problem. In the latter case we disregard states with more than one electron on any of the molecular site 1 and 2 so we need to consider only 9 bridge states: $|0_{1g}, 0_{2g}, 0_{1e}, 0_{2e}\rangle$, $|0_{1g}, 0_{2g}, 1_{1e}, 1_{2e}\rangle$ and $|1_{1g}, 1_{2g}, 0_{1e}, 0_{2e}\rangle$ in subspaces I; $|0_{1g}, 0_{2g}, 0_{1e}, 1_{2e}\rangle$, $|0_{1g}, 0_{2g}, 1_{1e}, 0_{2e}\rangle$, $|0_{1g}, 1_{2g}, 0_{1e}, 0_{2e}\rangle$ and $|1_{1g}, 0_{2g}, 0_{1e}, 0_{2e}\rangle$ in subspaces II; $|1_{1g}, 0_{2g}, 0_{1e}, 1_{2e}\rangle$ and $|0_{1g}, 1_{2g}, 1_{1e}, 0_{2e}\rangle$ in subspace III.

The diagonalization procedure yields the transformation between the eigenstates of the wire Hamiltonian and the states of the non-interaction molecular wire, $|n_{1g}, n_{2g}, n_{1e}, n_{2e}\rangle$ displayed in Fig.2. Denoting the column vectors of these states by $\{\Phi\}$ and $\{\chi\}$, respectively, and the transformation between them by \hat{Y} , i.e. $\{\chi\} = \hat{Y}\{\Phi\}$, we can characterized each eigenstate Φ by the corresponding subspace (λ_e, λ_g) . In this basis, the fermionic interaction picture operators (see Eq.(9)) read, for example

if $f = g$. $\tilde{\chi}$ denotes the transpose matrix $\hat{\chi}$. The relaxation terms in the master equation (8) take in this basis the forms

$$\begin{aligned} -\frac{1}{\hbar^2} Tr_K \int_0^\infty dx [\hat{V}, [\hat{V}^{int}(-x), \rho(t)]]_{\alpha\beta} &= \frac{1}{2} \sum_{nf\alpha'\beta'} \Gamma_{nf} \{ \hat{c}_{nf,\alpha\alpha'} \sigma_{\alpha'\beta'} \hat{c}_{nf,\beta'\beta}^+ [2 - f_{K_n}(E_{\beta'} - E_\beta) \\ &- f_{K_n}(E_{\alpha'} - E_\alpha)] + \hat{c}_{nf,\alpha\alpha'}^+ \sigma_{\alpha'\beta'} \hat{c}_{nf,\beta'\beta} [f_{K_n}(E_\beta - E_{\beta'}) + f_{K_n}(E_\alpha - E_{\alpha'})] - \{ \hat{c}_{nf,\alpha\alpha'} \hat{c}_{nf,\alpha'\beta'}^+ f_{K_n}(E_{\alpha'} - E_{\beta'}) \\ &+ \hat{c}_{nf,\alpha\alpha'}^+ \hat{c}_{nf,\alpha'\beta'} [1 - f_{K_n}(E_{\beta'} - E_{\alpha'})] \} \sigma_{\beta'\beta} - \sigma_{\alpha\alpha'} \{ \hat{c}_{nf,\alpha'\beta'} \hat{c}_{nf,\beta'\beta}^+ f_{K_n}(E_{\beta'} - E_{\alpha'}) + \hat{c}_{nf,\alpha'\beta'}^+ \hat{c}_{nf,\beta'\beta} [1 - f_{K_n}(E_{\alpha'} - E_{\beta'})] \} \} \end{aligned} \quad (27)$$

where

$$\Gamma_{nf} = \frac{2\pi}{\hbar} \sum_{k \in K_n} |V_k^{(nf)}|^2 \delta(\varepsilon_k - \varepsilon_{nf}) \quad (28)$$

and

$$\begin{aligned}
& -\frac{1}{\hbar^2} \text{Tr}_K \int_0^\infty dx [\hat{W}, [\hat{W}^{int}(-x), \rho(t)]]_{\alpha\beta} \\
& = \frac{1}{2} \sum_{n\alpha'\beta'} \{ -B_{K_n} [E_{\beta'}(\lambda_e + 1, \lambda_g) - E_{\alpha'}(\lambda_e, \lambda_g + 1), \mu_{K_n}] [b_{n,\alpha\alpha'}^+ b_{n,\alpha'\beta'} \sigma_{\beta'\beta}(t) + \sigma_{\alpha\beta'}(t) b_{n,\beta'\alpha'}^+ b_{n,\alpha'\beta}] \\
& \quad - B_{K_n} [E_{\alpha'}(\lambda_e, \lambda_g + 1) - E_{\beta'}(\lambda_e + 1, \lambda_g), \mu_{K_n}] [b_{n,\alpha\beta} b_{n,\beta'\alpha'}^+ \sigma_{\alpha'\beta}(t) + \sigma_{\alpha\alpha'}(t) b_{n,\alpha'\beta'} b_{n,\beta'\alpha'}^+] \\
& \quad + b_{n,\alpha\alpha'}^+ \sigma_{\alpha'\beta'}(t) b_{n,\beta'\beta} B_{K_n} [E_{\beta'}(\lambda_e, \lambda_g + 1) - E_{\beta}(\lambda_e + 1, \lambda_g), \mu_{K_n}] \\
& \quad + b_{n,\alpha\alpha'} \sigma_{\alpha'\beta'}(t) b_{n,\beta'\beta}^+ B_{K_n} [E_{\beta'}(\lambda_e + 1, \lambda_g) - E_{\beta}(\lambda_e, \lambda_g + 1), \mu_{K_n}] \\
& \quad + b_{n,\alpha\alpha'}^+ \sigma_{\alpha'\beta'}(t) b_{n,\beta'\beta} B_{K_n} [E_{\alpha'}(\lambda_e, \lambda_g + 1) - E_{\alpha}(\lambda_e + 1, \lambda_g), \mu_{K_n}] \\
& \quad + b_{n,\alpha\alpha'} \sigma_{\alpha'\beta'}(t) b_{n,\beta'\beta}^+ B_{K_n} [E_{\alpha'}(\lambda_e + 1, \lambda_g) - E_{\alpha}(\lambda_e, \lambda_g + 1), \mu_{K_n}] \}
\end{aligned} \tag{29}$$

where

$$B_{K_n}(E_\alpha - E_\beta, \mu_{K_n}) = \frac{2\pi}{\hbar} \sum_{k \neq k' \in K_n} |W_{kk'}^{(n)}|^2 \delta(\varepsilon_k - \varepsilon_{k'} + E_\alpha - E_\beta) f_{K_n}(\varepsilon_k) [1 - f_{K_n}(\varepsilon_{k'})] \tag{30}$$

In evaluating these forms we have taken the wide band limit for the electrodes spectral densities.

Next consider the diagonalization procedure itself. In subspaces I the unitary transformation $\hat{Y}(\lambda_e, \lambda_g)$ is obviously the unity matrix. The diagonalization of the block matrices in subspaces II and III is carry out in the limiting cases of zero and infinite on-site interactions.

A. Zero on site coupling

The case of zero on site coupling is discussed in Appendix A. We find the eigenfunctions and energies of the 2-site bridge summarized in Table I

	$\lambda_g = 0$	$\lambda_g = 1$	$\lambda_g = 2$
$\lambda_e = 0$	$\Phi(0, 0) = 0_{1g}, 0_{2g}, 0_{1e}, 0_{2e}\rangle$ $E = 0$	$\Phi_+(0, 1) = 0_{1g}, 1_{2g}, 0_{1e}, 0_{2e}\rangle$ $\Phi_-(0, 1) = 1_{1g}, 0_{2g}, 0_{1e}, 0_{2e}\rangle$ $E = 0$	$\Phi(0, 2) = 1_g, 1_{2g}, 0_e, 0_{2e}\rangle$ $E = 0$
$\lambda_e = 1$	$\Phi_\pm(1, 0) = \frac{1}{\sqrt{2}}(0_{1g}, 0_{2g}, 0_{1e}, 1_{2e}\rangle \mp 0_{1g}, 0_{2g}, 1_{1e}, 0_{2e}\rangle)$ $E = \varepsilon_{2e} \pm \Delta_e$ $\hat{\chi}(1, 0) = \begin{pmatrix} 0_{1g}, 0_{2g}, 0_{1e}, 1_{2e}\rangle \\ 0_{1g}, 0_{2g}, 1_{1e}, 0_{2e}\rangle \end{pmatrix}$	$\hat{\Phi}(1, 1) = Y^+(1, 1) \hat{\chi}(1, 1)$ $E = \frac{1}{2}(\varepsilon_{1e} + \varepsilon_{2e}) \pm \frac{1}{2}J\hbar \pm \frac{1}{2}\sqrt{4\Delta_e^2 + J^2\hbar^2}$ $\hat{\chi}(1, 1) = \begin{pmatrix} 1_{1g}, 0_{2g}, 1_{1e}, 0_{2e}\rangle \\ 1_{1g}, 0_{2g}, 0_{1e}, 1_{2e}\rangle \\ 0_{1g}, 1_{2g}, 1_{1e}, 0_{2e}\rangle \\ 0_{1g}, 1_{2g}, 0_{1e}, 1_{2e}\rangle \end{pmatrix}$	$\Phi_\pm(1, 2) = \frac{1}{\sqrt{2}}(1_{1g}, 1_g, 0_{1e}, 1_e\rangle \mp 1_{1g}, 1_{2g}, 1_{1e}, 0_{2e}\rangle)$ $E = \varepsilon_{2e} \pm \Delta_e$ $\hat{\chi}(1, 2) = \begin{pmatrix} 1_g, 1_{2g}, 0_e, 1_{2e}\rangle \\ 1_g, 1_{2g}, 1_e, 0_{2e}\rangle \end{pmatrix}$
$\lambda_e = 2$	$\Phi(2, 0) = 0_{1g}, 0_{2g}, 1_{1e}, 1_{2e}\rangle$ $E = \varepsilon_{1e} + \varepsilon_{2e}$	$\Phi_+(2, 1) = 0_{1g}, 1_{2g}, 1_{1e}, 1_{2e}\rangle$ $\Phi_-(2, 1) = 1_{1g}, 0_{2g}, 1_{1e}, 1_{2e}\rangle$ $E = \varepsilon_{1e} + \varepsilon_{2e}$	$\Phi(2, 2) = 1_{1g}, 1_{2g}, 1_{1e}, 1_{2e}\rangle$ $E = \varepsilon_{1e} + \varepsilon_{2e}$

where

$$Y^+(1, 1) = \frac{1}{\sqrt{2}} \begin{pmatrix} \sin \tau & -\cos \tau & -\cos \tau & \sin \tau \\ \cos \tau & \sin \tau & \sin \tau & \cos \tau \\ \sin \tau & \cos \tau & -\cos \tau & -\sin \tau \\ \cos \tau & -\sin \tau & \sin \tau & -\cos \tau \end{pmatrix}, \tag{31}$$

and where τ is given by

$$\cos 2\tau = \frac{-J\hbar}{\sqrt{4\Delta_e^2 + J^2\hbar^2}} \text{ and } \sin 2\tau = \frac{2\Delta_e}{\sqrt{4\Delta_e^2 + J^2\hbar^2}} \tag{32}$$

The current in this case is found to be

$$\begin{aligned} \langle I \rangle = & -\frac{2e}{\hbar} \Delta_e \text{Im} \{ [\sigma_{32}(1, 1) + \sigma_{41}(1, 1)] \cos 2\tau \\ & + [\sigma_{31}(1, 1) - \sigma_{42}(1, 1)] \sin 2\tau - \sum_{\lambda_g=0,2} \sigma_{-+}(1, \lambda_g) \} \end{aligned} \quad (33)$$

Indices "+" and "-" in Eq.(33) correspond to the functions $\Phi_+(1, \lambda_g)$ and $\Phi_-(1, \lambda_g)$, respectively, in Table I. Indices 1, 2, 3 and 4 label the eigenstates of the wire Hamiltonian in subspace III. The corresponding energies are given by formulas $E_1 \equiv E_{-,+}$, $E_2 \equiv E_{-,-}$, $E_3 \equiv E_{+,-}$, $E_4 \equiv E_{+,+}$ where

$$E_{\pm,\pm} = \varepsilon_e \pm \frac{1}{2} J \hbar \pm \frac{1}{2} \sqrt{4\Delta_e^2 + J^2 \hbar^2} \quad (34)$$

B. Rotating-wave approximation

The calculation of the non-diagonal elements of the density matrix $\sigma_{\alpha\beta}(1, \lambda_g)$ in Eq.(33) for the current is essentially simplified for very weak wire-lead coupling when the coherent time-evolution dominates the dynamics of the wire electrons. This means that the largest time-scale of the coherent evolution, given by the smallest energy difference, and the dissipative time-scale, determined by the electron and energy transfer rates, Γ_{nf} and $B_{K_n}(E_\alpha - E_\beta, \mu_{K_n})$, respectively, are well separated, i.e., $\hbar\Gamma_{nf}, \hbar B_{K_n}(E_\alpha - E_\beta, \mu_{K_n}) \ll |E_\alpha - E_\beta|$ for $\lambda_e = 1$ and $\alpha \neq \beta$. Then for $\lambda_e = 1$ and $\alpha \neq \beta$, Eq.(8) is dominated by the first term on the RHS. Consequently, $\sigma_{\alpha\beta}(1, \lambda_g)$ can be calculated in the first order of $\hbar\Gamma_{nf}/(E_\alpha - E_\beta)$ and $\hbar B_{K_n}(E_\alpha - E_\beta, \mu_{K_n})/(E_\alpha - E_\beta)$. This constitutes the essence of a rotating-wave approximation (RWA) [11]. Within it, one can provide a closed expression for the reduced density matrix elements $\sigma_{\alpha\beta}$ and for the stationary current. We shall use the RWA below in Sec.V and Appendix B.

C. Strong Coulomb repulsion at sites

In the limit of strong Coulomb repulsion, U_m is assumed to be so large that at most one excess electron resides on each site. Thus, the available Hilbert space for uncoupled sites is reduced to three states $\hat{\chi}(0, 0) = |0_{1g}, 0_{2g}, 0_{1e}, 0_{2e}\rangle$, $\hat{\chi}(2, 0) = |0_{1g}, 0_{2g}, 1_{1e}, 1_{2e}\rangle$ and $\hat{\chi}(0, 2) = |1_{1g}, 1_{2g}, 0_{1e}, 0_{2e}\rangle$ for subspaces I; two states $\hat{\chi}(1, 0) = \begin{pmatrix} |0_{1g}, 0_{2g}, 0_{1e}, 1_{2e}\rangle \\ |0_{1g}, 0_{2g}, 1_{1e}, 0_{2e}\rangle \end{pmatrix}$ and $\hat{\chi}(0, 1) = \begin{pmatrix} |0_{1g}, 1_{2g}, 0_{1e}, 0_{2e}\rangle \\ |1_{1g}, 0_{2g}, 0_{1e}, 0_{2e}\rangle \end{pmatrix}$ for subspaces II; and the state $\hat{\chi}(1, 1) = \begin{pmatrix} |1_{1g}, 0_{2g}, 0_{1e}, 1_{2e}\rangle \\ |0_{1g}, 1_{2g}, 1_{1e}, 0_{2e}\rangle \end{pmatrix}$ for the now 2-dimensional subspace III. The unitary operators

$\hat{Y}^+(1, 0)$ and $\hat{Y}^+(0, 1)$ and the corresponding eigenstates and eigenvalues are defined by the same Eqs. (46), (47) and (48), respectively, as before (see Appendix A). The operator $\hat{Y}^+(1, 1)$ is reduced to (see Appendix B)

$$\hat{Y}^+(1, 1) = \frac{1}{\sqrt{2}} \begin{pmatrix} 1 & 1 \\ -1 & 1 \end{pmatrix} \quad (35)$$

$\hat{Y}^+(1, 1)$ is used to obtain the corresponding eigenstates $\hat{\Phi}(1, 1) = Y^+(1, 1)\hat{\chi}(1, 1)$ and eigenvalues $E_{1,2} = \varepsilon_e \mp J\hbar$.

Substituting Eq.(35) into Eq.(49) of Appendix A for the current, we get for $\Delta_g = 0$

$$\langle I \rangle = \frac{2e}{\hbar} \Delta_e \text{Im} \sigma_{-+}(1, 0) \quad (36)$$

V. CURRENT FROM THE ENERGY TRANSFER INTERACTION IN THE WIRE

In a recent paper [40] Galperin, Nitzan and Ratner have predicted the existence of non-Landauer current induced by energy transfer interactions between a bridge molecule and electron-hole excitations in the leads. Here we show that a similar non-Landauer current arises from the exciton type interaction J in the wire itself. For simplicity we limit ourselves to electron transfer interaction between the wire and the metal leads, Eq.(27), and disregard the corresponding excitation transfer, Eq.(29). Also for simplicity we consider a large bias limit in the Coulomb blockade case when $\mu_L > \varepsilon_e$ and $\mu_R < \varepsilon_g$, and the states $\varepsilon_e, \varepsilon_g$ are positioned rather far ($\gg k_B T, \hbar|J|, |\Delta_e|$) from the Fermi levels of both leads so that $f_L(\varepsilon) = 1$ and $f_R(\varepsilon) = 0$ can be taken on the RHS of Eq.(27). Finally, we disregard electron transfer interaction in the "g" channel, i.e. we take $\Delta_g = 0$. Landauer type current would be realized in channel "e" when it is isolated from channel "g", i.e. when $J = 0$, $\Gamma_{1g} = \Gamma_{2g} = 0$ and $\lambda_g = 0$. Solving Eqs. (8), (27) in the RWA approximation under these conditions and substituting the steady-state solution into Eq.(36), we get, using also the normalization condition $\sum_{\lambda_e=0,1,2} \text{Tr} \sigma(\lambda_e, 0) = 1$,

$$\langle I \rangle_{RWA} = -e \frac{\Gamma_{1e} \Gamma_{2e}}{\Gamma_{1e} + \Gamma_{2e}} \quad (37)$$

Eq.(37) describes the Landauer current and coincides with Eq.(21) of Ref.[11] (excluding the sign).

In fact, the current vanishes for $\Gamma_{1e} = \Gamma_{2e} = 0$ even when $\Gamma_{1g}, \Gamma_{2g} \neq 0$, since $\Delta_g = 0$ (see Fig.3). Such selective coupling to the leads could be obtained for the bridge made of a quadruple quantum dot where the lateral ones are strongly coupled to the leads [47, 48].

Consider now the case when $\Gamma_{1e} = \Gamma_{2e} = 0$; $\Gamma_{1g}, \Gamma_{2g} \neq 0$; $\Delta_g = 0$ and $J \neq 0$. For this case Eqs.(8), (27) together with Eq.(36) lead to

$$\langle I \rangle = -4e\Gamma_g J^2 \Delta_e^2 \frac{1 - [\sigma_{--}(0, 1) + \sigma(2, 0)]}{\Delta_e^2 \Gamma_g^2 + 16\Delta_e^2 J^2 + \hbar^2 \Gamma_g^2 J^2} \quad (38)$$

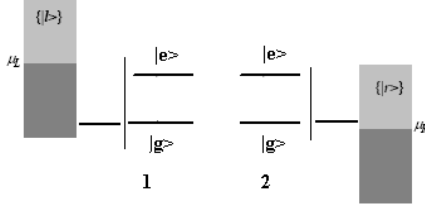


FIG. 3: A possible physical realization of the selective tunneling configuration, where only $|g\rangle$ levels are coupled to the leads.

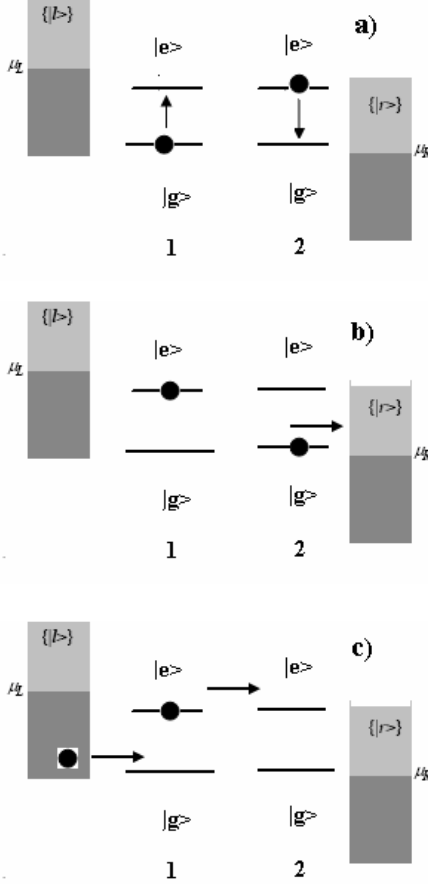


FIG. 4: Different stages of the energy-transfer induced current. a) energy transfer, $\sigma(1,1) \neq 0$. b) the charge transfer to the right lead. c) the intersite charge transfer, $\sigma(1,0) \neq 0$; the charge transfer from the left lead.

where for simplicity we put $\Gamma_{1g} = \Gamma_{2g} \equiv \Gamma_g$. Eq.(38) describes a non-Landauer current caused by transport in different channels: the intersite transfer occurs in channel "e", and the charge transfer between the molecular bridge and the leads occurs in channel "g". The inter-channel mixing is induced by the energy-transfer term J (see Fig.4). For example, starting with the molecular

system in state $|1_{1g}, 0_{2g}, 0_{1e}, 1_{2e}\rangle$, electron transmission takes place along route such as $|1_{1g}, 0_{2g}, 0_{1e}, 1_{2e}\rangle \xrightarrow{1} |0_{1g}, 1_{2g}, 1_{1e}, 0_{2e}\rangle \xrightarrow{2} |0_{1g}, 0_{2g}, 1_{1e}, 0_{2e}\rangle \xrightarrow{3} |0_{1g}, 0_{2g}, 0_{1e}, 1_{2e}\rangle \xrightarrow{4} |1_{1g}, 0_{2g}, 0_{1e}, 1_{2e}\rangle$. Step 1 is an energy transfer process, steps 2 and 3 rely on $\Gamma_{2g} \neq 0$ and $\Delta_e \neq 0$, respectively, and step 4 closes the circle via the Γ_{1g} process.

Eq.(38) clearly shows that the current exists only for $J \neq 0$ and $\Delta_e \neq 0$. For small J , $\langle I \rangle \sim J^2$. For large J we obtain

$$\langle I \rangle \simeq -4e\Gamma_g\Delta_e^2 \frac{1 - [\sigma_{--}(0,1) + \sigma(2,0)]}{16\Delta_e^2 + \hbar^2\Gamma_g^2} \quad (39)$$

which does not depend on J . In the limit $\hbar|J|, |\Delta_e| \gg \Gamma_g$, Eq.(38) yields for $\sigma_{--}(0,1) = \sigma(2,0) = 0$

$$\langle I \rangle_{RWA} = -\frac{e}{2} \frac{\Gamma_{2g}\Gamma_{1g}}{\Gamma_{2g} + \Gamma_{1g}} \quad (40)$$

In deriving Eq.(40) we have not put $\Gamma_{1g} = \Gamma_{2g}$. This limit corresponds to the range of validity of the RWA. Indeed, it can be shown that Eq. (40) can be obtained for this model in the RWA (see Appendix C).

If $\sigma_{--}(0,1), \sigma(2,0) \neq 0$, the non-Landauer current decreases, since the populations of states $|1_{1g}, 0_{2g}, 0_{1e}, 0_{2e}\rangle$ ($\sigma_{--}(0,1)$) and $|0_{1g}, 0_{2g}, 1_{1e}, 1_{2e}\rangle$ ($\sigma(2,0)$) suppress current. Two latter states are also steady-states in the case under consideration (Coulomb blocking, $\Gamma_{1e} = \Gamma_{2e} = \Delta_g = 0$) along with the states described by Fig.4. The existence of several steady-states corresponds to the presence of the respective zero eigenvalues of the relaxation matrix. Our numerical calculations give three such zero eigenvalues corresponding to three above steady-states.

If $\Gamma_{1e}, \Gamma_{2e} \neq 0$, state $|1_{1g}, 0_{2g}, 0_{1e}, 0_{2e}\rangle$ is only steady-state that "locks" the current due to Coulomb blocking, since $\Delta_g = 0$. Numerical simulations of other situations when $\Delta_g \neq 0$ and non-interacting electrons at a site are carried out in the next section.

VI. NUMERICAL RESULTS

The results presented in this section are based on direct numerical solution of Eq. (8), and are in complete agreement with the analytical solutions when applied to the special cases treated in Sections IV and V. The numerical solution was carried out using the basis of eigenstates of the Hamiltonian \hat{H}_{wire} , Eq.(3). Once $\sigma(t)$ is obtained from Eq. (8), the expectation value of the current is calculated as $\langle I \rangle = Tr(\hat{I}\sigma(t))$ where the current operator was defined by Eq.(26). In this calculation we have limited ourselves to the case where the wire-leads energy transfer coupling \hat{W} is disregarded and, unless otherwise specified, have used the following parameters: $\varepsilon_{1g} = \varepsilon_{2g} = 0.0eV$, $\varepsilon_{1e} = \varepsilon_{2e} = 2.0eV$, $\Delta_g = \Delta_e = 0.01eV$, $\Gamma_{1f} = \Gamma_{2f} = 0.02eV$ for $f = g, e$

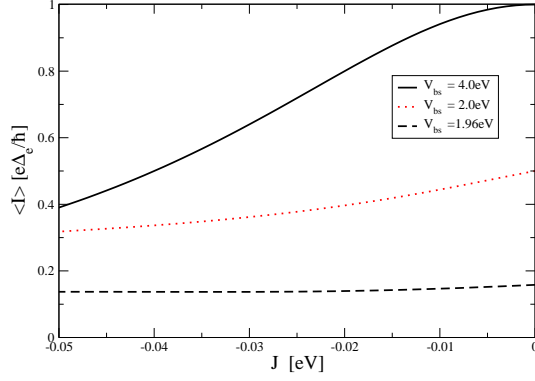


FIG. 5: The current $\langle I \rangle$ displayed as a function of the exciton coupling parameter J . $V_{bs} = 1.96\text{eV}$ (dashed line); $V_{bs} = 2.0\text{eV}$ (dotted line); $V_{bs} = 4.0\text{eV}$ (solid line)

(below we use Γ to denote the order of magnitude of these widths) and $T = 100\text{K}$. The Fermi levels were taken to align symmetrically with respect to the energy levels ε_{1g} and ε_{1e} , i.e. $\mu_L = (\varepsilon_{1g} + \varepsilon_{1e} + V_{bs})/2$ and $\mu_R = \mu_L - V_{bs}$. We also used the value of $e\Delta_e/\hbar = 2.45 \cdot 10^{-6}\text{A}$ as the unit of current $\langle I \rangle$.

Consider first non-interacting electrons. Figs.5, 6 and 7 show the expectation value of the current $\langle I \rangle$ and one-particle populations $P_{nf} = \text{Tr}(\hat{c}_{nf}^\dagger \hat{c}_{nf} \sigma)$ as functions of the exciton interaction parameter J . One can see that if the imposed voltage bias V_{bs} is larger than $\varepsilon_e - \varepsilon_g$, the expectation value of the current diminishes when $|J|$ increases (we have used $J < 0$ which is typical to J-aggregates, however the trend is similar with $J > 0$). Such a behavior can be understood, using Eq.(34) for the energies in subspaces (III) and Eq.(33) for the current. The latter equation shows two direct contributions to the current. The first one has its origin in states of subspace (III), the energies of which depend on both Δ_e and J (the first and the second terms on the RHS of Eq.(33)). The second contribution arises from states of subspaces (II), the energies of which depend on Δ_e only (the third terms on the RHS of Eq.(33)). Using Eqs.(8) with $\hat{W} = 0$ and (27), the non-diagonal elements of the density matrix on the RHS of Eq.(33) for the steady-state condition can be evaluated as $\sigma_{\alpha\beta} \sim \frac{-i\hbar\Gamma}{E_\alpha - E_\beta}$ (see also Sec.IV B). Since $E_- - E_+ = -2\Delta_e$, Eq.(48), we get for the contribution of the third term on the RHS of Eq.(33)

$$\frac{2e}{\hbar} \Delta_e \text{Im} \sum_{\lambda_g=0,2} \sigma_{-+}(1, \lambda_g) \sim 2e\Gamma \quad (41)$$

The contribution of the first and the second terms on the RHS of Eq.(33) depends on the relation between J and Δ_e .

When $\hbar|J| \ll \Delta_e$, Eq.(32) yields $\cos 2\tau \approx 0$, $\sin 2\tau \approx 1$, and only the second term in (33) gives a contribution to the current from the states of subspace (III). Under this condition one gets from Eq.(34) two doubly-degenerated

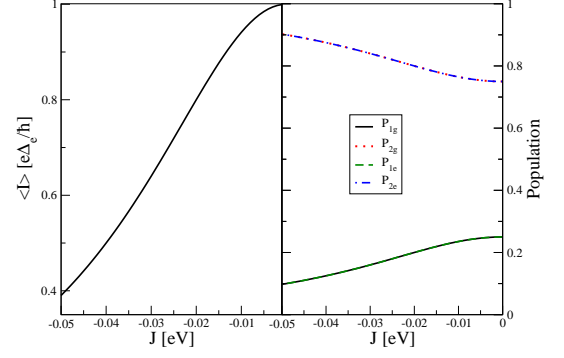


FIG. 6: The current $\langle I \rangle$ as a function of the parameter J in the case of non-interacting electrons for $V_{bs} = 4.0\text{eV}$. The current $\langle I \rangle$ is shown in left panel, and the populations P_{1g} , P_{1e} , P_{2g} and P_{2e} are shown in the right panel.

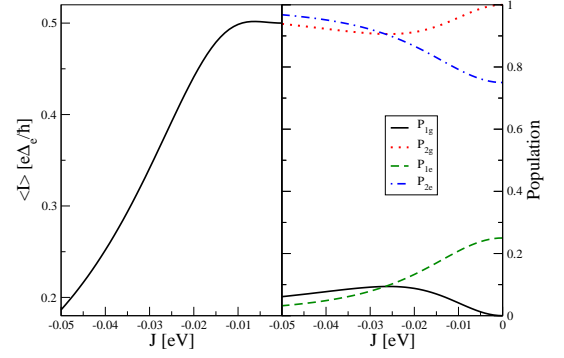


FIG. 7: Same as Fig.6 for the parameters $\Delta_g = 0$, $\Delta_e = 0.01\text{eV}$ and $V_{bs} = 4.0\text{eV}$.

values of energy $E_1 = E_4 = \varepsilon_e + \Delta_e$ and $E_2 = E_3 = \varepsilon_e - \Delta_e$, where the splitting is of the same order of magnitude as the hopping matrix element Δ_e . We obtain

$$\frac{2e}{\hbar} \Delta_e \text{Im}[\sigma_{31}(1, 1) - \sigma_{42}(1, 1)] \sim e\Gamma \quad (42)$$

This contribution is of the same order of magnitude as that from the states of subspaces (II).

In opposite case, $\hbar|J| \gg \Delta_e$, $\cos 2\tau \approx 1$ (again we use $J < 0$ -as in J-aggregates) and $\sin 2\tau \approx 0$. In this case only the first term in (33) contributes to the current from the states of subspace (III). For this case we get $E_2 \approx E_4 \approx \varepsilon_e$ and $E_{1,3} \approx \varepsilon_e \mp J\hbar$. This leads to

$$\frac{2e}{\hbar} \Delta_e \text{Im}[\sigma_{32}(1, 1) + \sigma_{41}(1, 1)] \sim e\Gamma \frac{\Delta_e}{J\hbar} \quad (43)$$

This contribution is much smaller than that of Eqs.(41) and (42), since the hopping matrix element Δ_e is much smaller than the splitting between states 3 and 2, and states 4 and 1 due to the exciton interaction (indices 1, 2, 3 and 4 label the the eigenstates of the wire Hamiltonian in subspace III). This can cause the value of the

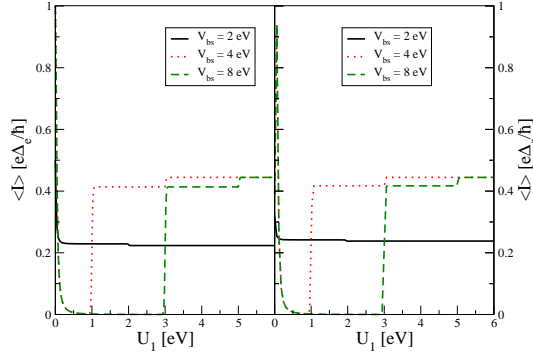


FIG. 8: The current $\langle I \rangle$ as a function of the Coulomb interaction parameter $U_1 = U_2$. $V_{bs} = 2.0\text{eV}$ (solid line); $V_{bs} = 4.0\text{eV}$ (dashed line); $V_{bs} = 8\text{eV}$ (dotted+dash line); $J = 0.0\text{eV}$ (left panel) and $J = -0.05\text{eV}$ (right panel).

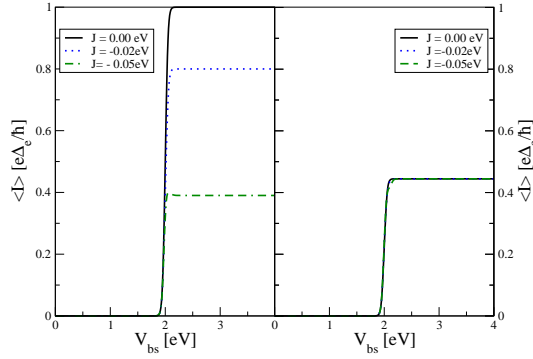


FIG. 9: The current $\langle I \rangle$ as a function of the bias voltage V_{bs} shown for different values of the exciton coupling parameter: $J = 0.0$ (solid line), $J = -0.02\text{eV}$ (dotted line), $J = -0.05\text{eV}$ (dash-dotted line). Left panel - noninteracting electrons. Right panel $U_1, U_2 = \infty$.

total current to decrease. In other words, the transitions $3 \rightarrow 2$ and $4 \rightarrow 1$ do not participate in electron transfer due to their large splitting for $\hbar|J| \gg \Delta_e$. This is in a sense “exciton blocking” of electron transmission through the bridge.

Next we turn to situations where electron-electron interaction is taken into account. Fig.8 shows the current $\langle I \rangle$ as a function of the Coulomb interaction parameter $U_1 = U_2$. Fig.9 depicts the current $\langle I \rangle$ as a function of the bias voltage V_{bs} for different values of the exciton coupling J for the case of non-interacting electrons as well as for the case of infinite on-site interaction between electrons. The “exciton blocking” effect seen for non-interacting electrons (smaller current for larger $|J|$) disappears in the case of Coulomb blocking.

This is supported by Eq.(36) that does not show a direct contribution of the states of subspace (III) to the current, and the above evaluation of the term $\frac{2e}{\hbar} \Delta_e \text{Im} \sigma_{-+}(1, 0)$. The point is that in the case of interacting electrons, subspace (III) includes only states,

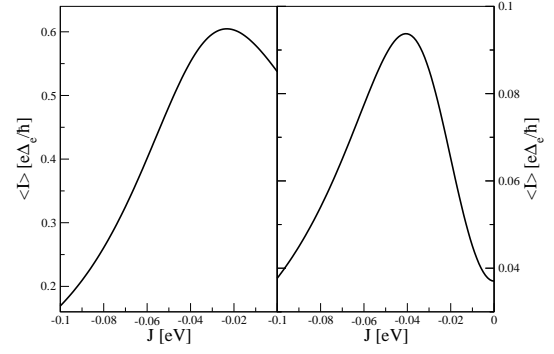


FIG. 10: The current $\langle I \rangle$ plotted against the exciton coupling parameter for bias $V_{bs} = 4.0\text{eV}$ for different energies in the e -channel: $\varepsilon_{1e} = 1.95\text{eV}$ and $\varepsilon_{2e} = 2.05\text{eV}$. $\Delta_g = 0.01\text{eV}$ (left panel), $\Delta_g = 0$ (right panel).

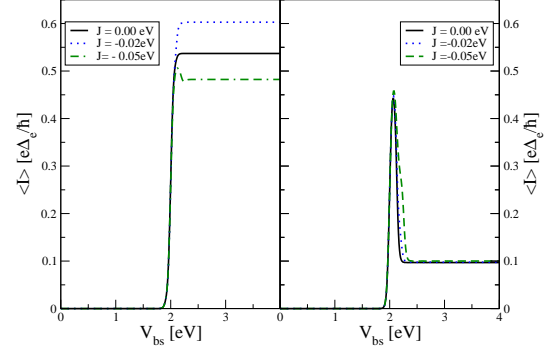


FIG. 11: Same as Fig. 9 except that $\varepsilon_{1e} = 1.95\text{eV}$ and $\varepsilon_{2e} = 2.05\text{eV}$.

which are acted upon exciton interaction (see Fig.2). Moreover, in the case of Coulomb blocking, the effect of exciton-induced current exists (Sec.V).

The effect of “exciton blocking” depends on the energy detuning $\varepsilon_{2f} - \varepsilon_{1f}$ in channel “ f ” for a heterodimer bridge. Figs.10 and 11 show the current $\langle I \rangle$ as a function of J for $\varepsilon_{2e} - \varepsilon_{1e} = 0.1\text{eV}$. $\langle I \rangle$ is seen to increase for small $|J|$, then to decrease as $|J|$ becomes larger. This can be related to the modification of resonance conditions when $\varepsilon_{2e} - \varepsilon_{1e} \neq 0$.

Finally, figures 12, 13, 14 and 15 show more of the system behavior for the model with $U_1, U_2 = \infty$. Fig.12 shows the current as a function of $|J|$ for different values of the imposed voltage bias V_{bs} . If V_{bs} is large compared to the energy difference between the excited and ground site energies, the current behaves in accordance with Eq.(38). If V_{bs} is close to this energy difference, the current increases initially with $|J|$, and then decreases to zero. Furthermore, in accordance with Eq.(38), the left panel of Fig.13 shows that the steady-state current is zero for the initial condition $\sigma_{--}(0, 1) = 1$. The steady-state current is zero also for the initial condition $\sigma(0, 0) = 1$, since the latter state relaxes to $\sigma_{--}(0, 1) = 1$. Figures 14

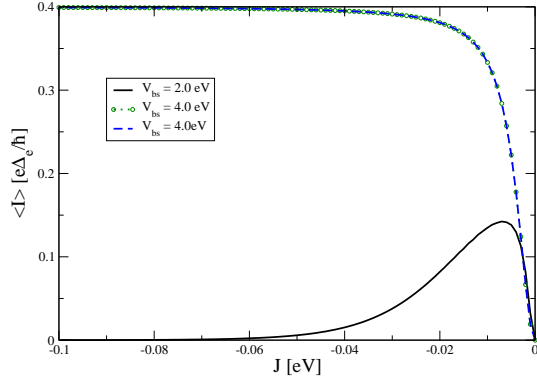


FIG. 12: Current as a function of $|J|$ for the initial population of state $|01g, 02g, 11e, 02e\rangle$ equal to 1. $\Delta_g = 0.0$, $\Delta_e = 0.01eV$, $\Gamma_{1g} = \Gamma_{2g} = 0.02eV$, $\Gamma_{1e} = \Gamma_{2e} = 0$. $V_{bs} = 2.0eV$ (solid line), $V_{bs} = 4.0eV$ (circles - numerical simulations, dashed - calculations with Eq.(38)).

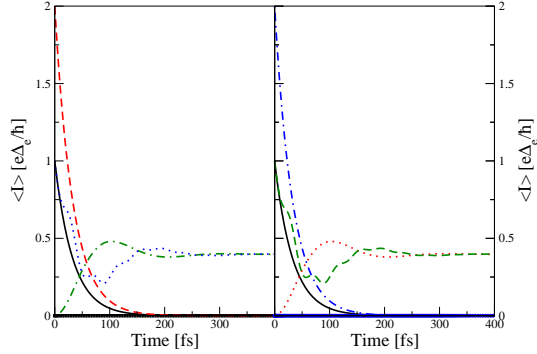


FIG. 13: Current $\langle I \rangle$ as a function of time for different initially populated many-electron states: $|01g, 02g, 01e, 02e\rangle$ - solid, $|11g, 02g, 01e, 02e\rangle$ - dashed, $J = -0.05eV$ and $V_{bs} = 8.0eV$. Left panel: $\Delta_g = 0$, $\Delta_e = 0.01eV$, $\Gamma_{1g} = \Gamma_{2g} = 0.02eV$, $\Gamma_{1e} = \Gamma_{2e} = 0$, $|01g, 02g, 01e, 12e\rangle$ - dot-dashed, $|01g, 12g, 01e, 02e\rangle$ - squares, $|01g, 02g, 11e, 02e\rangle$ - dotted. Right panel: $\Delta_g = 0.01eV$, $\Delta_e = 0$, $\Gamma_{1g} = \Gamma_{2g} = 0$, $\Gamma_{1e} = \Gamma_{2e} = 0.02eV$, $|01g, 02g, 11e, 02e\rangle$ - dot-dashed, $|01g, 12g, 01e, 02e\rangle$ - dotted, $|01g, 02g, 01e, 12e\rangle$ - squares.

and 15 show the time dependence of the current and one-particle populations for different initial conditions corresponding to the absence of relaxation in e -channel and g -channel, respectively.

VII. CONCLUSION

We have developed a theory of electron transport through a molecular wire in the presence of the effect of dipolar energy-transfer interaction between the sites in the wire. We found that such interaction, which leads to exciton excitations in the wire, cannot in general be disregarded. We used a model comprising a two two-level sites bridge connecting free electron reservoirs. Ex-

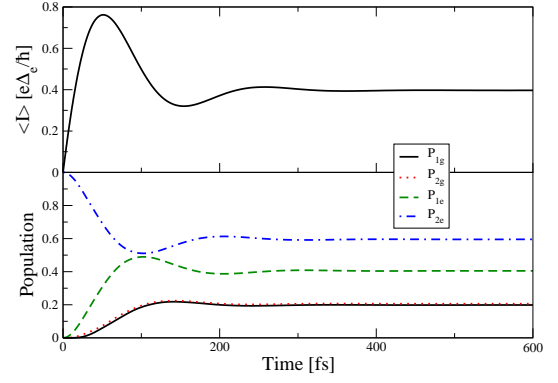


FIG. 14: Current and one-particle populations $P_{nf} = Tr(\hat{c}_{nf}^+ \hat{c}_{nf'} \sigma)$ as functions of time for the initial population of state $|01g, 02g, 01e, 12e\rangle$ equal to 1. $J = -0.05eV$, $V_{bs} = 8.0eV$, $\Delta_g = 0.0$, $\Delta_e = 0.01eV$, $\Gamma_{1g} = \Gamma_{2g} = 0.01eV$, $\Gamma_{M,1e} = \Gamma_{2e} = 0.0$.

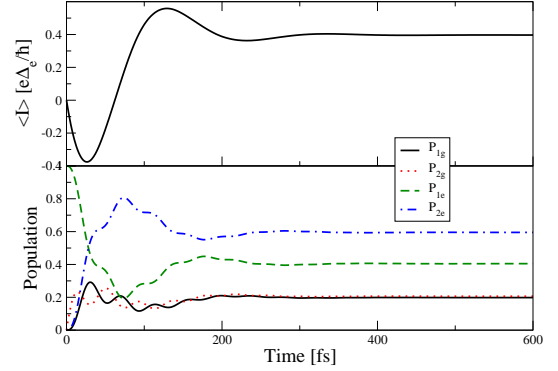


FIG. 15: Current and one-particle populations $P_{nf} = Tr(\hat{c}_{nf}^+ \hat{c}_{nf'} \sigma)$ as functions of time for the initial population of state $|01g, 02g, 11e, 02e\rangle$ equal to 1. $J = -0.05eV$, $V_{bs} = 8.0eV$, $\Delta_g = 0.0$, $\Delta_e = 0.01eV$, $\Gamma_{1g} = \Gamma_{2g} = 0$, $\Gamma_{1e} = \Gamma_{2e} = 0.02eV$.

panding the density operator in the many-electron eigenstates of the uncoupled sites, we obtain a 16×16 density matrix in the bridge subspace whose dynamics is governed by Liouville equation that takes into account interactions on the bridge as well as electron injection and damping to and from the leads. Our consideration has been considerably simplified by using the pseudospin description based on the symmetry properties of Lie group $SU(2)$. We studied the influence of the bias voltage, the Coulomb repulsion and the energy-transfer interactions on the steady-state current and in particular focus on the effect of the excitonic interaction between bridge sites. Our calculations show that in the case of non-interacting electrons this interaction leads to reduction in the current at high voltage for a homodimer bridge. This effect can be called “exciton” blocking. The effect of “exciton” blocking is modified for a heterodimer bridge, and disappears for strong Coulomb repulsion at sites. In the

latter case the exciton type interactions can open new channels for electronic conduction. In particular, in the case of strong Coulomb repulsion, conduction exists even when the electronic connectivity as defined above does not exist.

To end this discussion we note that in this work we have investigated a molecular bridge connecting metal leads. It is worthy to note that the geometry considered could modify the effect of dipolar energy-transfer interaction between the sites in the wire [26]. This issue will be considered elsewhere.

Acknowledgement

This work was supported by the German-Israeli Fund (PH, SK and AN), European Research Commission and the Israel Science Foundation (AN), the Israel-US binational Science Foundation (AN and BF), the Russia-Israel Scientific Research Cooperation (BF), the Deutsche Forschungsgemeinschaft through SPP 1243 and the German Excellence Initiative via the “Nanosystems Initiative Munich (NIM)” (PH, SK and BF).

VIII. APPENDIX A. NON-INTERACTING ELECTRONS AT A SITE

The unitary transformations $\hat{Y}(\lambda_e, \lambda_g) = I$ for subspaces (I). As to subspaces (II), Hamiltonian corresponding to the second line of the RHS of Eq.(24) where $\lambda_f = 1 \neq \lambda_{f'}$ ($f' \neq f$) can be diagonalized, using the unitary transformation

$$\begin{pmatrix} R_1^f \\ R_2^f \\ R_3^f \end{pmatrix} = \hat{T}^f \begin{pmatrix} r_1^f \\ r_2^f \\ r_3^f \end{pmatrix} \equiv \begin{pmatrix} \cos 2\vartheta_f & 0 & -\sin 2\vartheta_f \\ 0 & 1 & 0 \\ \sin 2\vartheta_f & 0 & \cos 2\vartheta_f \end{pmatrix} \begin{pmatrix} r_1^f \\ r_2^f \\ r_3^f \end{pmatrix} \quad (44)$$

where

$$\begin{aligned} \cos 2\vartheta_f &= \frac{\varepsilon_{2f} - \varepsilon_{1f}}{\sqrt{(\varepsilon_{2f} - \varepsilon_{1f})^2 + 4\Delta_f^2}}, \\ \sin 2\vartheta_f &= \frac{-2\Delta_f}{\sqrt{(\varepsilon_{2f} - \varepsilon_{1f})^2 + 4\Delta_f^2}} \end{aligned} \quad (45)$$

The matrix elements of \hat{T}^f are connected with the unitary transformations $\hat{Y}(\lambda_e, \lambda_g)$ for subspaces (II) by formula $T_{nj}^f = (1/2)Tr(\hat{\sigma}_n \hat{Y}^+ \hat{\sigma}_j \hat{Y})$ where $\hat{\sigma}_n$ and $\hat{\sigma}_j$ are Pauli matrices.

A. Unitary transformations for subspaces (II)

Consider subspaces (II). In the limit $U_m = 0$, the matrix \hat{T}^f , Eq.(44), with matrix elements $T_{nj}^f = (1/2)Tr[\hat{\sigma}_n \hat{Y}^+(\lambda_f = 1; \lambda_{f'} = 0, 2) \hat{\sigma}_j \hat{Y}(\lambda_f = 1; \lambda_{f'} = 0, 2)]$ describes a rotation by mixing angle $2\vartheta_f$ around axis “y”. $\hat{Y}(\lambda_f = 1; \lambda_{f'} = 0, 2)$ is an unitary operator

defined by

$$\hat{Y}^+(\lambda_f = 1; \lambda_{f'} = 0, 2) = \begin{pmatrix} \cos \vartheta_f & \sin \vartheta_f \\ -\sin \vartheta_f & \cos \vartheta_f \end{pmatrix} \quad (46)$$

which enables us to obtain eigenstates

$$\begin{pmatrix} \Phi_+(\lambda_f = 1; \lambda_{f'} = 0, 2) \\ \Phi_-(\lambda_f = 1; \lambda_{f'} = 0, 2) \end{pmatrix} = \hat{Y}^+(\lambda_f = 1; \lambda_{f'} = 0, 2) \times \hat{\chi}(\lambda_f = 1; \lambda_{f'} = 0, 2) \quad (47)$$

and eigenvalues

$$\begin{aligned} E_{\pm}(\lambda_f = 1; \lambda_{f'} = 0, 2) &= \frac{1}{2}[\lambda_e(\varepsilon_{1e} + \varepsilon_{2e}) + (\varepsilon_{2f} - \varepsilon_{1f}) \\ &\pm \sqrt{(\varepsilon_{2f} - \varepsilon_{1f})^2 + 4\Delta_f^2}] \end{aligned} \quad (48)$$

for subspaces (II). Here the many-electron eigenstates of the uncoupled sites are given by $\hat{\chi}(1, 0) = \begin{pmatrix} |0_{1g}, 0_{2g}, 0_{1e}, 1_{2e}\rangle \\ |0_{1g}, 0_{2g}, 1_{1e}, 0_{2e}\rangle \end{pmatrix}$, $\hat{\chi}(0, 1) = \begin{pmatrix} |0_{1g}, 1_{2g}, 0_{1e}, 0_{2e}\rangle \\ |1_{1g}, 0_{2g}, 0_{1e}, 0_{2e}\rangle \end{pmatrix}$, $\hat{\chi}(1, 2) = \begin{pmatrix} |1_{1g}, 1_{2g}, 0_{1e}, 1_{2e}\rangle \\ |1_{1g}, 1_{2g}, 1_{1e}, 0_{2e}\rangle \end{pmatrix}$ and $\hat{\chi}(2, 1) = \begin{pmatrix} |0_{1g}, 1_{2g}, 1_{1e}, 1_{2e}\rangle \\ |1_{1g}, 0_{2g}, 1_{1e}, 1_{2e}\rangle \end{pmatrix}$.

Taking the expectation value of the current, Eq.(26), we get

$$\begin{aligned} \langle I \rangle &= \frac{2e}{\hbar} \left\{ \sum_{\lambda_{f'}=0,2;f} \Delta_f \text{Im} \sigma_{-+}(\lambda_f = 1; \lambda_{f'}) - \sum_{\alpha\beta} \text{Im} \sigma_{\beta\alpha}(1, 1) \right. \\ &\quad \times [\hat{Y}^+(1, 1) \hat{\chi}^+(1, 1) (\Delta_e b_e + \Delta_g b_g) \tilde{\chi}(1, 1) \hat{Y}(1, 1)]_{\alpha\beta} \left. \right\} \end{aligned} \quad (49)$$

where we put $r_2^f = R_2^f$ for $\lambda_f = 1$ and $\lambda_{f'} = 0, 2$ that follows from Eq.(44) and used $\langle R_2^f(\lambda_f = 1; \lambda_{f'} = 0, 2) \rangle = Tr(\hat{\sigma}_2 \sigma) = 2\text{Im} \sigma_{-+}(\lambda_f = 1; \lambda_{f'} = 0, 2)$. Indices “+” and “-” in Eq.(49) correspond to the functions $\Phi_+(1, \lambda_g)$ and $\Phi_-(1, \lambda_g)$, respectively, in Table I.

B. Unitary transformation for subspace (III)

The calculation of $\hat{Y}^+(1, 1)$ is more involved. Consider for brevity a homodimer bridge with $\varepsilon_{ng} = 0$, $\varepsilon_{ne} = \varepsilon_e$ and $\Delta_g = 0$. Bearing in mind future generalizations of our model to N -sites, we shall transform the Paulion operators (b_f^+, b_f) to fermion operators (β_f^+, β_f) through the Jordan-Wigner transformation [41, 49, 50]:

$$\begin{aligned} \beta_e &= b_e, \quad \beta_e^+ = b_e^+, \quad \beta_g = \exp(i\pi b_e^+ b_e) b_g, \\ \beta_g^+ &= b_g^+ \exp(-i\pi b_e^+ b_e) \end{aligned} \quad (50)$$

Then \hat{H}_{wire} , Eqs.(3) and (20), can be rewritten for subspace (III) in terms of the fermion operators as

$$\hat{H}_{wire}(\lambda_e = \lambda_g = 1) = \varepsilon_e - \Delta_e(\beta_e^+ + \beta_e) - \hbar J(\beta_e^+ \beta_g + \beta_g^+ \beta_e) \quad (51)$$

Eq.(51) is a quadratic in Fermi operators and can be diagonalized in two stages. Its "excitonic" part $\hat{H}_{ex} = -\hbar J(\beta_e^+ \beta_g + \beta_g^+ \beta_e)$ is readily transformed to satisfy the condition $\hat{H}_{ex} = \sum_j \hbar \epsilon_j a_j^+ a_j$ if we take [49]

$$\begin{aligned} a_j &= \sqrt{2/3}(\beta_g \sin \frac{\pi j}{3} + \beta_e \sin \frac{2\pi j}{3}), \\ \epsilon_j &= -2J \cos \frac{\pi j}{3}, \quad j = 1, 2 \end{aligned} \quad (52)$$

where a_j are also Fermi operators. The corresponding occupation number basis set contains $2^2 = 4$ eigenfunctions of the system. The single-excited states are given by $a_j^+ |0\rangle = \sum_f \phi_{jf} |f\rangle = \sqrt{1/2}(|g\rangle + (-1)^{j-1} |e\rangle)$

where $|0\rangle \equiv |1_{1g}, 0_{2g}, 1_{1e}, 0_{2e}\rangle$ is the "vacuum" state, and $|g\rangle \equiv |0_{1g}, 1_{2g}, 1_{1e}, 0_{2e}\rangle$ and $|e\rangle \equiv |1_{1g}, 0_{2g}, 0_{1e}, 1_{2e}\rangle$ are the states with the corresponding donor acceptor pair excited. The eigenstate with two excitations can be written down in terms of the Slater determinant

$$a_{j_1}^+ a_{j_2}^+ |0\rangle = \begin{vmatrix} \phi_{j_1 e} & \phi_{j_1 g} \\ \phi_{j_2 e} & \phi_{j_2 g} \end{vmatrix} |eg\rangle = \frac{1}{2}[(-1)^{j_2} - (-1)^{j_1}] |eg\rangle \quad (53)$$

with energy $\epsilon_1 + \epsilon_2 = 0$ equal to that of the vacuum state where $|eg\rangle \equiv |0_{1g}, 1_{2g}, 0_{1e}, 1_{2e}\rangle$. The wire Hamiltonian can be written down in terms of a_j as $\hat{H}_{wire}(\lambda_e = \lambda_g = 1) = \epsilon_e + \sum_j \hat{H}_j$ where $\hat{H}_j = \hat{F}_j + (-1)^j \hbar J a_j^+ a_j$, $\hat{F}_j = (-1)^j (\Delta_e / \sqrt{2})(a_j^+ + a_j)$ is the "hopping" operator with the only nonzero matrix elements involving states which differ by a single excitation: $\langle 0 | \hat{F}_j a_j^+ | 0 \rangle = (-1)^j \Delta_e / \sqrt{2}$, $\langle 0 | a_{j_2} \hat{F}_{j_1} a_{j_1}^+ a_{j_2}^+ | 0 \rangle = (-1)^{j_1} \Delta_e / \sqrt{2}$. The eigenstates and eigenvalues of $\hat{H}_{wire}(\lambda_e = \lambda_g = 1)$ can be calculated now as follows. $\hat{\Phi}(1, 1) = Y^+(1, 1) \hat{\chi}(1, 1)$ where $Y^+(1, 1)$ is

given by Eqs.(31) and (32), $\hat{\chi}(1, 1) = \begin{pmatrix} |0\rangle \\ |e\rangle \\ |g\rangle \\ |eg\rangle \end{pmatrix}$, and

$$\begin{aligned} \hat{\Phi}(1, 1) &= \frac{1}{\sqrt{2}} \begin{pmatrix} (|0\rangle + |eg\rangle) \sin \tau - (|e\rangle + |g\rangle) \cos \tau \\ (|e\rangle + |g\rangle) \sin \tau + (|0\rangle + |eg\rangle) \cos \tau \\ (|e\rangle - |g\rangle) \cos \tau + (|0\rangle - |eg\rangle) \sin \tau \\ (|0\rangle - |eg\rangle) \cos \tau - (|e\rangle - |g\rangle) \sin \tau \end{pmatrix} \\ &\equiv \begin{pmatrix} |\Phi_1\rangle \\ |\Phi_2\rangle \\ |\Phi_3\rangle \\ |\Phi_4\rangle \end{pmatrix} \end{aligned} \quad (54)$$

Substituting Eq.(31) into Eq.(49) for the current, we get Eq.(33) for $\Delta_g = 0$.

IX. APPENDIX B. UNITARY TRANSFORMATION FOR SUBSPACE (III) FOR INTERACTING ELECTRONS AT A SITE

In the limit of strong Coulomb repulsion, the operator $\hat{Y}^+(1, 1)$ is reduced to that defined by Eq.(35) in accordance with Eqs.(52), since the "hopping" operator $\hat{F}_j = (-1)^j (\Delta_e / \sqrt{2})(a_j^+ + a_j)$ has no nonzero matrix elements involving states with a single excitation $|e\rangle$ and $|g\rangle$ (see Appendix A).

Substituting Eq.(35) into Eq.(49) for the current, we get Eq.(36) for $\Delta_g = 0$.

X. APPENDIX C

The steady-state solution of Eqs. (8), (27) in the RWA approximation gives for the case under consideration

$$\sigma(0, 0) = \sigma(0, 2) = \sigma_{++}(0, 1) = \sigma_{+-}(0, 1) = \sigma_{-+}(0, 1) = 0 \quad (55)$$

and $\sigma_{--}(0, 1)$ and $\sigma(2, 0)$ are arbitrary. Putting $\sigma_{--}(0, 1) = \sigma(2, 0) = 0$, we get

$$\sigma_{-+}(1, 0) = \frac{i\hbar}{-8\Delta_e} \{ \Gamma_{M,1g} Tr \sigma(1, 0) + \Gamma_{M,2g} Tr \sigma(1, 1) \} \quad (56)$$

and $Tr \sigma(1, 0) = (\Gamma_{M,2g} / \Gamma_{M,1g}) Tr \sigma(1, 1)$. Then using the normalization condition

$$Tr \sigma(1, 0) + Tr \sigma(1, 1) = 1 \quad (57)$$

and Eq.(36), we obtain Eq.(40) of Sec.V.

-
- [1] A. Nitzan and M. A. Ratner, Science **300**, 1384 (2003).
 - [2] M. Galperin, M. A. Ratner, A. Nitzan, and A. Troisi, Science **319**, 1056 (2008).
 - [3] F. Chen and N. J. Tao, Accounts of Chemical Research **42**, 429 (2009).

- [4] J. R. Heath, Annual Review of Materials Research **39**, 1 (2009).
- [5] M. D. Ventra, S. T. Pantelides, and N. D. Lang, Phys. Rev. Lett. **84**, 979 (2000).
- [6] J. Heurich, J. C. Cuevas, W. Wenzel, and G. Schon, Phys.

- Rev. Lett. **88**, 256803 (2002).
- [7] F. Evers, F. Weigend, and M. Koentopp, Phys. Rev. B **69**, 235411 (2004).
 - [8] Y. Xue, S. Datta, and M. A. Ratner, Chem. Phys. **281**, 151 (2002).
 - [9] P. Damle, A. W. Ghosh, and S. Datta, Chem. Phys. **281**, 171 (2002).
 - [10] S. Kohler, J. Lehmann, and P. Hanggi, Phys. Reports **406**, 379 (2005).
 - [11] F. J. Kaiser, M. Strass, S. Kohler, and P. Hanggi, Chem. Phys. **322**, 193 (2006).
 - [12] Y. Meir and N. S. Wingreen, Phys. Rev. Lett. **68**, 2512 (1992).
 - [13] M. Galperin, M. A. Ratner, and A. Nitzan, J. Phys.: Condens. Matter **19**, 103201 (2007).
 - [14] A. S. Davydov, *Theory of Molecular Excitons* (Plenum, New York, 1971).
 - [15] V. M. Agranovich, *Teoriya Excitonov* (Nauka, Moscow, 1968).
 - [16] D. P. Craig and S. H. Walmsley, *Excitons in molecular crystals* (Benjamin, New York, 1968).
 - [17] V. M. Agranovich and A. A. Zakhidov, Chem. Phys. Lett. **50**, 278 (1977).
 - [18] M. Hoffmann *et al.*, Chem. Phys. **258**, 73 (2000).
 - [19] C. Warns, I. J. Lalov, and P. Reineker, Journal of Luminescence **129**, 1840 (2009).
 - [20] J. R. G. Thorne, S. T. Repinec, S. A. Abrash, and R. M. Hochstrasser, Chem. Phys. **146**, 315 (1990).
 - [21] A. Tilgner, H. P. Trommsdorff, J. M. Zeigler, and R. M. Hochstrasser, J. Chem. Phys. **96**, 781 (1992).
 - [22] M. Shimizu *et al.*, J. Luminescence **87–89**, 933 (2000).
 - [23] A. C. Benniston, A. Harriman, P. Li, and C. A. Sams, J. Am. Chem. Soc. **127**, 2553 (2005).
 - [24] O.-K. Kim, J. Je, and J. S. Melinger, J. Am. Chem. Soc. **128**, 4532 (2006).
 - [25] J. Tang, Y. Wang, C. Nuckolls, and S. J. Wind, J. Vac. Sci. Technol. B **24**, 3227 (2006).
 - [26] J. I. Gersten and A. Nitzan, Chem. Phys. Lett. **104**, 31 (1984).
 - [27] X. M. Hua, J. I. Gersten, and A. Nitzan, J. Chem. Phys. **83**, 3650 (1985).
 - [28] H. Mertens, A. F. Koenderink, and A. Polman, Phys. Rev. B **76**, 115123 (2007).
 - [29] H. Mertens and A. Polman, J. Appl. Phys. **105**, 044302 (2009).
 - [30] G. P. Wiederrecht, G. A. Wurtz, and J. Hranisavljevic, Nanoletters **4**, 2121 (2004).
 - [31] G. A. Wurtz *et al.*, Nanoletters **7**, 1297 (2007).
 - [32] N. I. Cade, T. Ritman-Meer, and D. Richards, Phys. Rev. B **79**, 241404(R) (2009).
 - [33] I. Bondarev, L. M. Woods, and K. Tatur, Phys. Rev. B **80**, 085407 (2009).
 - [34] K. L. Kelly, E. Coronado, L. L. Zhao, and G. C. Schatz, J. Phys. Chem. B **107**, 668 (2003).
 - [35] K. Li, M. I. Stockman, and D. J. Bergman, Phys. Rev. Lett. **91**, 227402 (2009).
 - [36] V. A. Markel, J. Phys. B: At. Mol. Opt. Phys. **38**, L347 (2005).
 - [37] F. Wang and Y. R. Shen, Phys. Rev. Lett. **97**, 206806 (2006).
 - [38] T. Brixner *et al.*, Phys. Rev. B **73**, 125437 (2006).
 - [39] M. Sukharev and T. Seideman, J. Phys. B: At. Mol. Opt. Phys. **40**, S283 (2007).
 - [40] M. Galperin, A. Nitzan, and M. A. Ratner, Phys. Rev. Lett. **96**, 166803 (2006).
 - [41] E. Fradkin, *Field theories of condensed matter systems* (Addison-Wesley, New York, 1991).
 - [42] S. Welack, M. Schreiber, and U. Kleinekathofer, J. Chem. Phys. **124**, 044712 (2006).
 - [43] T. Novotny, Europhys. Lett. **59**, 648 (2002).
 - [44] L. Allen and J.-H. Eberly, *Optical resonance and two-level atoms* (John Wiley & Sons, New York, London, Sydney, Toronto, 1975).
 - [45] F. T. Hioe and J. H. Eberly, Phys. Rev. Lett. **47**, 838 (1981).
 - [46] Z. S. Yang, N. H. Kwong, and R. Binder, Phys. Rev. B **70**, 195319 (2004).
 - [47] T. Bryllert *et al.*, Appl. Phys. Letters **80**, 2681 (2002).
 - [48] R. Sanchez, G. Platero, and T. Brandes, Phys. Rev. B **78**, 125308 (2008).
 - [49] D. B. Chesnut and A. Suna, J. Chem. Phys. **39**, 146 (1963).
 - [50] F. C. Spano, Phys. Rev. Lett. **24**, 3424 (1991).